

Functional identification of an aggression locus in the mouse hypothalamus

Dayu Lin^{1,2,5}, Maureen P. Boyle³, Piotr Dollar⁴, Hyosang Lee¹, Pietro Perona⁴, Ed S. Lein³, and David J. Anderson^{1,2,5}

¹Division of Biology 216-76, California Institute of Technology, 1200 East California Boulevard, Pasadena, California 91125

²Howard Hughes Medical Institute, Seattle, Washington, USA

³Allen Institute for Brain Science, Seattle, Washington, USA

⁴Computation and Neural Systems 136-93, California Institute of Technology, 1200 East California Boulevard, Pasadena, California 91125

Abstract

Electrical stimulation of certain hypothalamic regions in cats and rodents can elicit attack behavior, but the exact location of relevant cells within these regions, their requirement for naturally occurring aggression and their relationship to mating circuits have not been clear. Genetic methods for neural circuit manipulation in mice provide a potentially powerful approach to this problem, but brain stimulation-evoked aggression has never been demonstrated in this species. Here we show that optogenetic, but not electrical, stimulation of neurons in the ventromedial hypothalamus, ventrolateral subdivision (VMHvl) causes male mice to attack both females and inanimate objects, as well as males. Pharmacogenetic silencing of VMHvl reversibly inhibits inter-male aggression. Immediate early gene analysis and single unit recordings from VMHvl during social interactions reveal overlapping but distinct neuronal subpopulations involved in fighting and mating. Neurons activated during attack are inhibited during mating, suggesting a potential neural substrate for competition between these behaviors.

A central problem in neuroscience is to understand how instinctive behaviors¹, such as aggression, are encoded in the brain. Classic experiments in cats have demonstrated that attack behavior can be evoked by electrical stimulation of the hypothalamus²⁻³. However the precise location of the relevant neurons, and their relationship to circuits for other instinctive social behaviors, such as mating, remain unclear. Studies in the rat have identified a broadly distributed “hypothalamic attack area” (HAA)⁴⁻⁸ that partially overlaps

Users may view, print, copy, download and text and data-mine the content in such documents, for the purposes of academic research, subject always to the full Conditions of use: http://www.nature.com/authors/editorial_policies/license.html#terms

⁵Authors for correspondence.

AUTHOR CONTRIBUTIONS

D. Lin designed, carried out and analyzed preliminary fos catFISH experiments and all other experiments, and co-wrote the manuscript; M. Boyle and E. Lein performed additional fos catFISH experiments; P. Dollar and P. Perona developed custom behavior annotation software; H. Lee performed some of the optogenetic experiments; D.J. Anderson conceived project, suggested experiments, analyzed data and co-wrote the manuscript.

several anatomic nuclei⁹. In contrast, neurons involved in predator defense and mating appear to respect the boundaries of specific, and complementary, hypothalamic nuclei¹⁰⁻¹¹. How aggression circuits are related to these two behavioral subsystems⁹⁻¹⁰ remains poorly understood (but see ref. 12). Immediate early gene (IEG) mapping experiments have suggested that aggression and mating involve similar limbic structures¹³⁻¹⁵, but whether this reflects the involvement of the same or different cells within these structures is not clear.

We have investigated the localization of hypothalamic neurons involved in aggression, and their relationship to neurons involved in mating, in the male mouse. Using a combination of genetically based functional manipulations and electrophysiological methods, we identify an aggression locus within the ventrolateral subdivision of VMH (VMHvl)⁹. Surprisingly, this structure also contains distinct neurons active during male-female mating. Many neurons activated during aggressive encounters are inhibited during mating. These data suggest a close neuroanatomical relationship between aggression and reproductive circuits, and a potential neural substrate for competition between these social behaviors¹.

RESULTS

Intermingled mating and fighting neurons

We first employed conventional non-isotopic analysis of *c-fos* induction, a surrogate marker of neuronal excitation¹⁶, to map activity during offensive aggression in the resident-intruder test¹⁷. For comparison, we performed a similar analysis during mating with females. Mating and fighting induced *c-fos* mRNA in the medial amygdala, medial hypothalamus and bed nucleus of the stria terminalis (BNST; Fig. S1), as previously described in rats and hamsters^{13,15}, but not in the anterior hypothalamic nucleus (AHN) which has been implicated in aggression by many studies¹⁸⁻¹⁹ (reviewed in ref 20). While the pattern of mating vs. fighting-induced *c-fos* was similar in most structures, such between-animal comparisons do not distinguish whether these social behaviors activate the same or different neurons.

To address this issue, we adapted a method, called cellular compartment analysis of temporal activity by fluorescent *in situ* hybridization (catFISH)²¹⁻²² to compare *c-fos* expression induced during two consecutive behavioral episodes in the same animal (Figs. 1a-f). We examined four limbic regions (VMHvl, ventral premammillary nucleus (PMv), medial amygdala posterodorsal (MEApd) and posteroventral (MEApv)) that exhibited strong *c-fos* induction in single-labeling experiments (Fig. S1). Animals sacrificed immediately after 5 min of fighting had almost exclusively nuclear *c-fos* transcripts, while those sacrificed 35 minutes after fighting had essentially only cytoplasmic transcripts (Fig. S2). In animals that engaged in two successive episodes of the same behavior separated by 30 min, most cells expressing nuclear *c-fos* transcripts also expressed cytoplasmic *c-fos* mRNA (Figs. 1c, d, g and S3, green and red bars), indicating activation during both behavioral episodes. By contrast, in animals that sequentially engaged in two different behaviors, only 20-30% of cells with nuclear *c-fos* RNA also expressed cytoplasmic *c-fos* transcripts (Figs. 1e, f, g and S3, blue and magenta bars). (Nevertheless, the overlap between nuclear and cytoplasmic *c-fos* hybridization was slightly greater than expected by chance

even when the two sequential behaviors were different (Fig. S4)). These results suggest, firstly, that the same neurons are likely to be recruited during two successive episodes of mating or fighting, even though such neurons are relatively sparse (Fig. S5, < 12% of total cells *c-fos*⁺); and secondly, that mating and fighting may recruit overlapping but distinct sets of neurons in these brain regions.

Chronic recording from the VMHvl

To gain further insight into the relationship between neurons active during mating and fighting, we performed chronic single-unit recordings in awake, behaving male mice using a 16-wire electrode bundle²³ (see Methods). We selected VMHvl for these studies, because it showed preferential *c-fos* induction after fighting vs. mating (Fig. S5; aggression-induced *c-fos* in VMHvl was further confirmed by double labeling for *c-fos* and *vglut2*, a glutamate transporter enriched in VMH; Fig. S6), and because it overlaps partially with the rat HAA7. Recording from VMHvl is challenging because of its deep location, and small size; in only 5 of 30 implanted animals were all 16 electrode tracks confined to VMHvl (Fig. S7). Neurons excited during social behaviors (Fig. 2h, red dots) were rarely found from the 25 mis-targeted animals. We successfully recorded from 104 well-isolated cells in the 5 VMHvl-targeted animals. By holding the same cell during alternating, sequential exposures to female and male stimulus animals (Figs. 2a and S8), we could distinguish whether the unit was activated by males and/or females (see Methods for unit isolation criteria).

Neuronal activity patterns in VMHvl during social encounters showed diverse temporal dynamics and sex-selectivity (Figs. 2, 3, S8 and S9). Spontaneous firing rates prior to introduction of the stimulus animal were typically low (median = 1.1 Hz, range 0-12.7 Hz) and rarely increased during home cage behaviors (i.e. grooming); some cells were completely silent until the stimulus animal was presented. Spiking activity was correlated with behavior by computer-assisted manual annotation of videotape (see Methods). Over 50% (53/104) of recorded cells increased their firing rate during at least one behavioral episode of a social encounter (Fig. 3c). A large fraction (41%; 43/104) of VMHvl cells exhibited increased firing during an encounter with a male stimulus animal, and on average spiking activity increased with escalation of the encounter, independent of intruder strain (Fig. 3e). In many cases (19/43) this increase began as soon as the intruder male was introduced, and continued as the social encounter progressed, while in a comparable number increased firing was observed only during close investigation and subsequent attack (Figs. 2b-d, middle plots, and 3a; Movie S1). Strikingly, a small subset of cells (12%; 5/43) was excited exclusively during attack (Figs. 2e, middle plot, and 2g).

In contrast, during encounters with females, spiking activity in VMHvl tended to increase only transiently during the initial investigative phase, and subsequently declined as mating progressed (Fig. 3e). Among 35 cells that were excited during female investigation, almost two-thirds (23/35) decreased their firing during subsequent mounting (Figs. 2b and f; left, right; Fig. 3b), and 7 were suppressed (below their baseline firing rate) during thrust and ejaculation (Figs. 2f, right, S9c and d). Almost half (25/53) of all activated cells were excited by both males and females, although most of the largest increases in activity were in sex-specific cells (see Footnote S1 and Fig. S10). Furthermore most of this overlap was

transitory, occurring during the initial stages of the social encounter and diminishing as the interaction progressed to the consummatory phase of attack or copulation. The observation of partially overlapping populations of male- and female-excited cells in VMHvl qualitatively confirms the results of our fos catFISH studies (Fig. S10 and Footnote S1). However, the evolving segregation of the two populations as the social encounters progressed was not anticipated by the IEG analysis, due to its insufficient temporal resolution.

Our electrophysiological recordings also revealed that the majority (14/18) of male-excited cells were actively suppressed (below their baseline firing rates) during encounters with females (Figs. 2c, 3c, 3d, S8a, c, e and g; Movie S2). Most (86%; 12/14) of those cells, moreover, responded to male intruders prior to any physical contact. This observation suggests that cells excited during the initiation of an aggressive encounter are selectively suppressed during interactions with a female. In contrast, of the 10 cells selectively excited by females, only 2 were actively suppressed during a male-male encounter (Fig. 2f, middle). This asymmetry in sex-specific inhibitory responses indicates that suppression of fighting-related neurons during mating is more pronounced than the converse.

Optogenetic stimulation induced attack

We next tested whether functional manipulations of VMHvl would affect mating or fighting. Although VMHvl overlaps the rat HAA7-8,24, extensive attempts to elicit attack by conventional electrical stimulation of this region in mice were unsuccessful (see Footnote S2, Fig. S11). As an alternative, therefore, we expressed Channelrhodopsin-2 (ChR2) in VMHvl neurons unilaterally, using stereotactic co-injection of adeno-associated viral vectors (AAV2) expressing Cre recombinase and a Cre-dependent form of ChR2-EYFP25-26, and selectively illuminated cells in this region using an implanted fiber-optic cable²⁷ (Fig. 4a). Because AAV2 infects neurons preferentially²⁸ (Fig. S12) and does not retrogradely infect cells from their axons or nerve terminals²⁹, only neurons whose cell bodies are local to the injection site express ChR2 (Footnote S3). Optotrode recording in anaesthetized animals confirmed that ChR2 expressing cells in VMH can be driven to fire with high temporal precision (Fig. S13). Consistent with this result, c-fos could be strongly induced in VMHvl on the infected, but not the contralateral control side after repeated blue light stimulation in awake behaving animals (Figs. 4b-e).

Optogenetic stimulation of VMHvl in the absence of an intruder did not obviously alter behavior, except for an occasional increase in exploratory activity. In contrast, in the presence of an intruder, illumination elicited a rapid onset of coordinated and directed attack, often towards the intruder's back (Movie S3, see Methods for more detailed behavior description). Importantly, whereas male mice rarely spontaneously attack females or castrated males, 11/16 ChR2-expressing males exhibited attack towards such intruder animals, within 4-5 seconds after the onset of illumination (Fig. 4l), over multiple trials (Fig. 4k, Test 1, blue bars). In 9/11 animals, attack was induced during a second test session 1-6 days later (Fig. 4k, Trial 2). Animals with low infection (<10 cells/section, N = 4) or animals injected with saline during the surgery (N = 4) showed no obvious behavioral changes during light stimulation.

Interestingly, upon illumination offset test animals ceased attack towards females significantly faster than towards castrated males (Fig. 4l, Attack offset). Furthermore, when low intensity (1 mW/mm^2) light was used, castrated males were attacked more readily than females (Fig. 4m). We also tested whether illumination could induce attack towards anaesthetized intruders or inanimate objects. Six of 10 animals attacked stationary anaesthetized animals upon illumination; all test animals attacked if the anaesthetized intruders were artificially moved (Fig. 4n). Two of 8 test animals attacked a stationary inflated glove, while 6/8 animals attacked if the glove was moved (Fig. 4n; Movie S4).

Histological analysis revealed that when the majority of infected cells was located in VMHvl, light stimulation effectively induced attack (red circles in Fig. 4p). In contrast, freezing and flight were observed when VMHdm and VMHc were infected to an equal or greater extent (green circles in Fig. 4p)30. Infection in other regions, such as VMHvl anterior, the lateral hypothalamic area (LHA) and tuberal nucleus (TU) was not associated with illumination-induced behavioral changes (Fig. S14 and S15, Footnote S4). To test more directly whether neurons in regions of the HAA8 surrounding VMHvl are sufficient to induce aggression, we deliberately infected such regions with AAV2-ChR2. No attack could be induced by light stimulation in such animals ($N = 5$). Strikingly, in cases where the AAV2-ChR2 spread into VMHvl, attack was induced ($N=3$) (Fig. S16). These data suggest that neurons located within VMHvl, but not in adjacent regions, play a key role in mouse aggression.

The observations that overall activity in VMHvl decreases during male-female mating (Fig. 3e), and that many male-excited cells are inhibited by females (Fig. 3d), suggested that a progressive inhibition of attack neurons occurs as mating progresses towards its consummatory phase. To test this, we stimulated VMHvl during encounters with females, prior to mounting, during intromission, between intromissions and after ejaculation. When illumination was delivered prior to mounting, attack towards the female was elicited in over 80% of trials at light intensities between $1-2\text{mW/mm}^2$, in all 7 tested animals (Fig. 4o, white bar). But during intromission, the same light intensity was often ineffective, even with extended stimulation (Fig. 4o, black bar). Increasing the light intensity 4-fold elicited female-direct attack during intromission in 5 of 7 animals, but with increased latency (Fig. S17). Between intromissions, attack was evoked in 30% of cases. Strikingly, following ejaculation the frequency of illumination-evoked attack recovered to pre-mounting levels (Fig. 4o, dark gray bar). Thus mating exerts an increasingly strong suppression of optogenetically stimulated attack, as the encounter progresses towards its consummatory phase.

Mouse aggression requires VMHvl activity

Whether neurons that mediate brain stimulation-evoked attack are also required for naturally occurring aggression has been controversial. Electrolytic lesions of VMH in rats and mice have yielded seemingly contradictory results31-32, and this method destroys axons-of-passage as well as cell bodies. There is little evidence that local chemical inhibition of neuronal activity in the rat HAA reduces aggression (although inhibition33 or killing34 of Substance P receptor-expressing neurons attenuates “hard biting” behavior). We therefore

HHMI Author Manuscript
HHMI Author Manuscript
HHMI Author Manuscript
asked whether reversible genetic suppression of electrical excitability in VMHvl neurons inhibits attack behavior. To do this, we used separate AAV2 vectors to co-express two subunits (α and β) comprising a *C. elegans* ivermectin (IVM)-gated chloride channel (GluCl $\alpha\beta$)35, which has been mutated to eliminate glutamate sensitivity36. Upon IVM binding, this heteropentameric channel prevents action potential firing by hyperpolarizing the membrane28,35.

Three weeks after viral injection, animals were administered IVM (i. p.) 24 hr prior to testing28. The experimental group ($n = 33$) exhibited a decrease in the total attack duration, and an increase in the latency to the first attack, in comparison to saline-injected or GluCl β -only injected controls (Figs. 5f & g; see Methods). Furthermore, 25% of the experimental animals failed to initiate any attack during the post-IVM test. Experimental animals performed similarly in the rotarod assay before and after IVM administration, indicating no change in motor coordination or fatigue (Fig. S18). Eight days after the IVM injection, the aggression level of the test group recovered to the pre-IVM level and could be suppressed again by a second IVM injection (Fig. 5h). Immunohistochemical analysis (Figs. 5a and d) indicated a reverse correlation between the suppression of aggression and the percentage of GluCl-expressing cells in the posterior half of VMHvl (Bregma level -1.4 — -1.75 mm; Fig. 5k). No such correlation was found in VMHvl anterior (Bregma level -1.15 — -1.4 mm) or in other regions surrounding VMHvl (Fig. S19). Double-label immunostaining for GFP and Fos in animals sacrificed 1 hr after an aggressive interaction (following IVM washout) indicated that viral infection overlapped the population activated during fighting ($[(GFP^+ \text{ Fos}^+)/\text{total Fos}^+] > 50\%$; $n = 4$; Figs. 5b-e). These data indicate that genetic silencing of neurons in VMHvl can reversibly inhibit aggressive behavior. In GluCl-expressing males paired with females, no change in mounting duration or latency to the first mount was observed after IVM injection (Figs. 5i and j). Since the overall level of neuronal activity in VMHvl is normally suppressed during the consummatory phase of mating (Fig. 3e), it is not surprising that further inhibition of activity failed to impair such behavior.

DISCUSSION

Using genetically based manipulations in mice, we show that neurons necessary and sufficient for offensive aggression are localized within a small subdivision of VMH. The more diffuse HAA identified in rats6,24 may reflect a species difference, or the fact that electrical stimulation mapping37 activates both axons-of-passage and neuronal somata, while our manipulations are restricted to the latter. Our *in vivo* recordings indicate that some neurons in VMHvl are activated by intruder conspecifics prior to physical contact. This suggests a function in olfactory coding, perhaps related to sex discrimination. However, optogenetic stimulation of VMHvl evoked aggressive behavior towards an inanimate object, arguing for a causal role in the motivation or drive to attack. We suggest that VMHvl plays a key role in sensori-motor transformations and/or the encoding of motivational states9 underlying aggression. The relationship of the aggression circuits within VMHvl to those involved in defensive12,20,38 or maternal39-40 aggression remains to be investigated.

While VMH is well established to play a key role in female reproductive behavior41-42, it has not traditionally been considered as a key node in male mating circuitry11 (but see13).

We have identified cells within the VMHvl of males that are activated during male-female mating, and which are mostly distinct from those activated during fighting. The role of these neurons is not yet clear, since our functional manipulations did not perturb mating behavior. One possibility is that these female-activated neurons serve to inhibit aggression during mating. Consistent with this idea, many male-activated units were actively inhibited by females, and a higher intensity of illumination was required to evoke attack towards a female during mating encounters. These data identify a neural correlate of competitive interactions between fighting and mating¹. Whether this competition originates in VMHvl, or is controlled by descending inputs to this nucleus⁴³, awaits further investigation.

METHODS SUMMARY

Sexually experienced C57BL/6N male mice, singly housed on a reverse light-dark cycle, were used. Resident-intruder assays were designed to maximize offensive aggression by the resident; no attacks were initiated by the intruder under our conditions. For *in situ* hybridization, animals were sacrificed 30 min after a 10 min standard resident-intruder assay and processed as described⁴⁴. For fos catFISH experiments, animals experienced two 5 min behavioral episodes 30 min apart, and were sacrificed immediately after the second episode. An intronic *c-fos* probe and a *c-fos* cRNA probe were combined to detect nuclear *c-fos* primary transcripts. For chronic recording, a movable bundle of sixteen 13-μm tungsten microwires was implanted, and 2 weeks allowed for recovery. On recording days, a flexible cable was attached to the microdrive and connected to a commutator. Recordings were performed in the animals' home cage. Female and male mice were introduced for approximately 10 min per session. Spiking activity and behavior were synchronously recorded. Data analysis, including behavioral annotation of videotapes, was performed using custom software written in Matlab. For ChR2 experiments, 150nl of a 4:2:1 mixture of an AAV2 Cre inducible EF1α::ChR226, AAV2 CMV::CRE and AAV2 CMV::LacZ with a similar final titer (8×10^{11} pfu/mL) was stereotactically injected unilaterally. After 2 weeks of recovery, light pulses (20 ms, 20 Hz, 1-4 mW/mm²) were delivered to activate the targeted region for 2-20sec in the presence of various stimuli. For GluCl inactivation experiments, animals in the experimental (bilateral injection of 10^9 AAV2 CAG::GluCl-CFP and CAG::GluClβ-YFP particles each side) and each of the three control groups (no surgery, saline or GluClβ bilaterally injected) were tested 3 times in the resident-intruder assay to establish a stable aggression baseline. After the third test, IVM (1%, 5mg/kg) was injected i. p. and the animals tested again 24 hr and 8 days later.

METHODS

Behavioral tests

All test animals used in this study were adult proven breeder C57BL/6 male mice (Charles River Laboratory). They were singly housed under a reversed light-dark cycle for at least 1 week before the test. The care and experimental manipulation of the animals were carried out in accordance with the NIH guidelines and approved by the Caltech Institutional Animal Care and Use Committee. For resident-intruder assays, C57BL/6 males were allowed to interact with BALB/c males for 10 min. All intruder mice were group housed, and had

similar body weight as the test mice. All resident animals included in the study initiated all the attacks and showed no submissive postures during the aggression test. For mating tests, the residents were allowed to interact with sexually receptive BALB/c and C57BL/6 females for 10 min. Females were screened for receptivity by pairing with a singly housed C57BL/6 male mouse briefly before each test.

In situ hybridization

Brains from mice sacrificed 30 minutes after performing either the 10 min resident-intruder or mating tests were analyzed for expression of *c-fos* mRNA throughout the forebrain, using non isotopic *in situ* hybridization on 120 μm -thick sections. Details of the procedure have been described previously⁴⁴. For *fos* catFISH experiments, animals experienced two consecutive 5 min fighting or mating episodes 30 min apart, and were sacrificed immediately after the second episode. Since *c-fos* transcripts are detected only in the nucleus within the first 5 minutes following induction, and are completely translocated to the cytoplasm as processed mRNA after 35 minutes, the sub-cellular location of *c-fos* allows one to distinguish neurons activated by a single stimulus from those successively activated by both stimuli: Only in the latter case will transcripts be present in both the nucleus and cytoplasm. We used an intronic *fos* probe with a different fluorescent color label, in addition to the *fos* cRNA probe, which allowed us to more easily differentiate nuclear from cytoplasmic FISH signals. The *c-fos* transcript distribution pattern was examined using both color combinations (*fos* cRNA probe in green and *fos* intronic probe in red, or vice versa) and no difference was observed. See Supplementary Methods for more detailed dFISH procedure and microscopic analysis.

Electrophysiological recording

A bundle of sixteen tungsten microwires (13 μm diameter each, California Fine Wire) attached to a mechanical microdrive was implanted in one hemisphere and secured with bone screws and dental acrylic during stereotactic surgery. The drive was a miniaturized version of an original design described elsewhere⁴⁵. Two weeks after initial implantation, and on days of recording, a flexible cable was attached to the microdrive and connected to a torqueless, feedback-controlled commutator (Tucker Davis Technology). During recording sessions, the test animals were allowed to stay in their home cage and interact with the stimulus animals freely. Female or male mice were introduced into the test arena for approximately 10 min. A given type of stimulus (e.g. a male mouse) was presented on multiple occasions, to examine the reproducibility of a response. All recordings were carried out in subdued light with infrared illumination. A commercial recording system was used for data acquisition (Tucker Davis Technology). Digital infrared video recordings of animal behavior from both side and top view were simultaneously streamed to a hard disk at 640 \times 480 pixel resolution at 25 frames per second (Streampix, Norpix). Each video frame acquisition was triggered by a TTL pulse from the recording setup to achieve synchronization between the video and the electrophysiological recording. Spikes of individual neurons were sorted using commercial software (OpenSorter, Tuck Davis Technology), based on principal component analysis. Unit isolation was verified using autocorrelation histograms. To ensure that single units were isolated, and that the same units were recorded in the presence of sequentially presented male or female stimulus animals, we

imposed four criteria to select cells for subsequent statistical analysis. First, the cells had to have a signal/noise ratio > 3; second, the spike shape had to be stable throughout the recording; third, the response had to be repeatable during multiple trials; fourth, the percentage of spikes occurring with inter-spike intervals (ISIs) < 3 ms (the typical refractory period for a neuron) in a continuous recording sequence had to be < 0.1%. 74 out of 104 cells included in the analysis had all of their ISIs < 3 ms. After each recording session, the microwire bundle was advanced 70 μ m, by adjusting a 00-90 screw on the drive 1/4 turn. After 5 to 10 recording sessions, which typically were distributed over 2 to 3 months, animals were sacrificed and the location of the recording electrodes verified histologically.

Behavioral annotation and statistical analysis of firing rate changes

Custom software written in Matlab was used to facilitate manual annotation of mouse behavior from videotaped recording sessions. Annotations were made using side- and top-view videos played simultaneously. A total of ~1000 10 min videos were carefully analyzed on a frame-by-frame basis. The behavioral results were then correlated with the electrophysiology to obtain histograms of firing rates during various behavioral episodes. Firing rates for each unit were averaged in 0.5 sec bins, and the mean firing rate during each behavioral episode (e.g. "Investigation") was compared to the baseline firing rate (i.e., prior to introduction of the test animals) using Kruskal-Wallis one-way analysis of variance by ranks (with p value 0.01), followed by a pairwise test for significance with Tukey-Kramer correction for multiple comparisons, to determine whether there was any statistically significant change in activity during a given episode. If the same stimulus was tested multiple times, only repeatable responses were regarded as positive.

ChR2 viral activation

The Cre-inducible EF1 α ::ChR2-EYFP construct was the generous gift of K. Deisseroth and was described earlier⁴⁶. Since ChR2 is a membrane protein expressed mainly in axons, we co-injected an AAV2 CMV::LacZ virus to facilitate the quantification and anatomic localization of infected cells. AAV2 CMV::CRE and AAV2 CMV::LacZ viruses were purchased from Vectorbiolabs. AAV2 CRE inducible EF1 α ::ChR2-EYFP virus was prepared by the Harvard Vector Core Facility. The AAV2-ChR2, AAV2-CRE and AAV2-LacZ viruses were mixed in a 4:2:1 volume ratio to reach a similar final titer (8×10^{11} pfu/mL). A total of 0.15 μ l of the mixed virus suspension (approximately 1.2×10^8 particles) was injected unilaterally over a period of 5 minutes using a fine glass capillary (Nanoject II, Drummond Scientific). After injection, a 24 gauge cannula (Plastics One) was inserted and secured to a depth of approximately 0.6 mm above the target region (Metabond, Parkell). After 2 weeks recovery, and on test days, a 200 μ m multimode optical fiber (Thorlabs) was inserted into the cannula and secured with an internal cannula adaptor and a cap (Plastics One). The tip of the fiber was cut flat to the bottom of the implanted cannula. Blue (473 nm) light was delivered in 20 ms pulses at 20 Hz, at final output powers ranging from 1 to 4 mW/mm² (CrystalLaser). Each light stimulation episode lasted from 2 to 20 seconds, depending on the behavioral responses. Initial tests using various frequencies indicated that 10-15 Hz was the minimal frequency necessary to induce a behavioral response. All animals were tested twice with 1 to 6 days between tests. Light induced attack typically includes the following steps: the stimulated animal approaches the intruder from a distance, bites the

intruder's back repeatedly, then either stops abruptly upon the cessation of light stimulation and moves away, or stops biting gradually after several rounds of attack. Light induced escape behavior typically includes the following steps: the stimulated animal makes a quick movement towards the corner of the arena. If the animal is engaged in other behaviors such as fighting or mating, it stops those behaviors and moves to a corner of the cage. Typically, the animal will stay in the corner and maintain the same posture for the remainder of the stimulation period.

One hour before sacrificing the animal, a train of light (10 sec on and 10 sec off, 20 ms, 20 Hz × 20) was delivered to induce Fos expression in the absence of any target animal. A total of 28 animals were implanted and tested. Twenty seven animals were processed for histological analysis and were included in the scatter plot of Fig. 4p. To quantify the extent of infection, we counted all the LacZ⁺ cells in various regions and calculated the number of LacZ⁺ cells in VMHvl posterior, VMHvl anterior, VMHdm + VMHc, LH and TU for each section. Fluorescent Nissl or NeuN staining was used to determine the boundaries of different VMH subdivisions. In cases where the boundary was hard to determine precisely, we delineated VMHvl as extending from the ventral pole of VMH approximately 1/3 of the way along the dorso-ventral and medio-lateral axes.

GluCl viral inactivation

Animals in the experimental group (n = 33) were stereotactically injected bilaterally with a total of 0.9 µl AAV2-GluClα and AAV2-GluClβ, each under the control of the CAG promoter-enhancer, in a 1:1 mixture (approximately 10⁹ particles), using a glass capillary attached to an auto nanoliter injector (Drummond). The viral constructs have been described previously²⁸. One control group received no surgery (n = 12), a second and third control group received either saline (n = 6) or AAV2-GluClβ (n = 12) during the surgery. After 2 weeks of recovery, the aggression level of the animal was evaluated using a 10 min resident-intruder assay 3 times on different days. After the third test, a 1% sterile solution of Ivermectin (Phenectin, AmTech) was injected (i.p.) at 5 mg/kg animal body weight. The animal were then tested again 24 hr and 8 days later. The effect of IVM typically wears off completely by 8 days²⁸ and any behavioral change is expected to be reversed at that time point. The mating test was performed using a similar procedure, except that a receptive female mouse was used as the stimulus animal. The rotarod assay was performed as described previously⁴⁷. The animal was exposed to a 10 min resident-intruder assay 1 hr before sacrifice to induce Fos expression. The brains were then harvested for histological analysis.

Supplementary Material

Refer to Web version on PubMed Central for supplementary material.

ACKNOWLEDGEMENTS

We thank S. Ciocchi, S. Lin, Y. Ben-Shaul and A. Wang for advice on electrode and microdrive design; M. Gerfen and M. Vondrus for microdrive fabrication; M.P. Walsh, T.D. Heitzman and V. Rush for electronics support; A. Steele, R. Robbins, S. Ossorio, K. Gunapala, A. Paul, D. Oh, C. Kim and J. Nishiguchi for behavior annotation and video scoring; H. Kim for technical assistance; W. E. Haubensak for teaching fiber-optic implant methods; J.T.

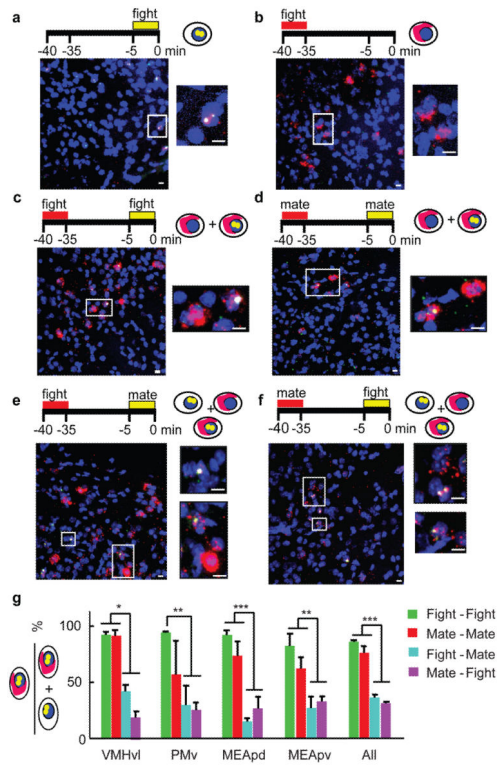
Henderson for advice on stereotactic surgery; M. Kruk for advice on electric stimulation experiment; G. Mosconi for lab management; K. Deisseroth for ChR2-EYFP construct. M. Kruk, R. Mooney and R. Simerly for comments on the manuscripts. This work was supported in part by the Weston-Havens Foundation and Jane Coffin Childs Foundation. D.J.A. is an Investigator of the Howard Hughes Medical Institute.

REFERENCES

1. Tinbergen, N. *The study of instinct*. Vol. xii. Clarendon Press/Oxford University Press; 1951.
2. Hess WR. Stammganglien-Reizversuche. Berichte der gesamten Physiologie. 1928; 42
3. Hess WR, Brügger M. Das subkortikale Zentrum der affektiven Abwehr-reaktion. *Helv. Physiol. Acta*. 1943; I:33–52.
4. Hrabovszky E, et al. Neurochemical characterization of hypothalamic neurons involved in attack behavior: glutamatergic dominance and co-expression of thyrotropin-releasing hormone in a subset of glutamatergic neurons. *Neuroscience*. 2005; 133:657–666. [PubMed: 15908131]
5. Kruk MR, et al. Discriminant analysis of the localization of aggression-inducing electrode placements in the hypothalamus of male rats. *Brain Res.* 1983; 260:61–79. doi: 0006-8993(83)90764-3 [pii]. [PubMed: 6681724]
6. Kruk MR. Ethology and pharmacology of hypothalamic aggression in the rat. *Neuroscience and biobehavioral reviews*. 1991; 15:527–538. [PubMed: 1792015]
7. Lammers JH, Kruk MR, Meelis W, van der Poel AM. Hypothalamic substrates for brain stimulation-induced attack, teeth-chattering and social grooming in the rat. *Brain research*. 1988; 449:311–327. [PubMed: 3395851]
8. Siegel A, Roeling TA, Gregg TR, Kruk MR. Neuropharmacology of brain-stimulation-evoked aggression. *Neuroscience and biobehavioral reviews*. 1999; 23:359–389. [PubMed: 9989425]
9. Swanson LW. Cerebral hemisphere regulation of motivated behavior. *Brain Res.* 2000; 886:113–164. doi:S0006-8993(00)02905-X [pii]. [PubMed: 11119693]
10. Canteras NS. The medial hypothalamic defensive system: hodological organization and functional implications. *Pharmacol Biochem Behav*. 2002; 71:481–491. [PubMed: 11830182]
11. Simerly RB. Wired for reproduction: organization and development of sexually dimorphic circuits in the mammalian forebrain. *Annual review of neuroscience*. 2002; 25:507–536.
12. Motta SC, et al. Dissecting the brain's fear system reveals the hypothalamus is critical for responding in subordinate conspecific intruders. *Proc Natl Acad Sci U S A*. 2009; 106:4870–4875. doi:0900939106 [pii]10.1073/pnas.0900939106. [PubMed: 19273843]
13. Kollack-Walker S, Newman SW. Mating and agonistic behavior produce different patterns of Fos immunolabeling in the male Syrian hamster brain. *Neuroscience*. 1995; 66:721–736. [PubMed: 7644033]
14. Newman SW. The medial extended amygdala in male reproductive behavior. A node in the mammalian social behavior network. *Annals of the New York Academy of Sciences*. 1999; 877:242–257. [PubMed: 10415653]
15. Veening JG, et al. Do similar neural systems subserve aggressive and sexual behaviour in male rats? Insights from c-Fos and pharmacological studies. *European journal of pharmacology*. 2005; 526:226–239. [PubMed: 16263109]
16. Morgan JI, Cohen DR, Hempstead JL, Curran T. Mapping patterns of c-fos expression in the central nervous system after seizure. *Science (New York, N.Y. 1987)*; 237:192–197.
17. Blanchard DC, Blanchard RJ. Ethoexperimental approaches to the biology of emotion. *Annual review of psychology*. 1988; 39:43–68.
18. Delville Y, De Vries GJ, Ferris CF. Neural connections of the anterior hypothalamus and agonistic behavior in golden hamsters. *Brain, behavior and evolution*. 2000; 55:53–76.
19. Ferris CF, Poteagal M. Vasopressin receptor blockade in the anterior hypothalamus suppresses aggression in hamsters. *Physiology & behavior*. 1988; 44:235–239. [PubMed: 2853382]
20. Nelson RJ, Trainor BC. Neural mechanisms of aggression. *Nature reviews*. 2007; 8:536–546.
21. Guzowski JF, McNaughton BL, Barnes CA, Worley PF. Imaging neural activity with temporal and cellular resolution using FISH. *Current opinion in neurobiology*. 2001; 11:579–584. [PubMed: 11595491]

22. Guzowski JF, McNaughton BL, Barnes CA, Worley PF. Environment-specific expression of the immediate-early gene Arc in hippocampal neuronal ensembles. *Nature neuroscience*. 1999; 2:1120–1124. [PubMed: 10570490]
23. Herry C, et al. Switching on and off fear by distinct neuronal circuits. *Nature*. 2008; 454:600–606. doi:nature07166 [pii]10.1038/nature07166. [PubMed: 18615015]
24. Roeling TA, et al. Efferent connections of the hypothalamic “aggression area” in the rat. *Neuroscience*. 1994; 59:1001–1024. [PubMed: 8058117]
25. Boyden ES, Zhang F, Bamberg E, Nagel G, Deisseroth K. Millisecond-timescale, genetically targeted optical control of neural activity. *Nature neuroscience*. 2005; 8:1263–1268. [PubMed: 16116447]
26. Kravitz AV, et al. Regulation of parkinsonian motor behaviours by optogenetic control of basal ganglia circuitry. *Nature*. 2010; 466:622–626. doi:nature09159 [pii]10.1038/nature09159. [PubMed: 20613723]
27. Aravanis AM, et al. An optical neural interface: in vivo control of rodent motor cortex with integrated fiberoptic and optogenetic technology. *Journal of neural engineering*. 2007; 4:S143–156. [PubMed: 17873414]
28. Lerchner W, et al. Reversible silencing of neuronal excitability in behaving mice by a genetically targeted, ivermectin-gated Cl⁻ channel. *Neuron*. 2007; 54:35–49. [PubMed: 17408576]
29. Taymans JM, et al. Comparative analysis of adeno-associated viral vector serotypes 1, 2, 5, 7, and 8 in mouse brain. *Human gene therapy*. 2007; 18:195–206. [PubMed: 17343566]
30. Lammers JH, Kruk MR, Meelis W, van der Poel AM. Hypothalamic substrates for brain stimulation-induced patterns of locomotion and escape jumps in the rat. *Brain research*. 1988; 449:294–310. [PubMed: 3395850]
31. Olivier B. Ventromedial hypothalamus and aggressive behavior in rats. *Aggressive Behavior*. 1977; 3:1.
32. Olivier B, Wiepkema PR. Behaviour changes in mice following electrolytic lesions in the median hypothalamus. *Brain research*. 1974; 65:521–524. [PubMed: 4472010]
33. Halasz J, et al. The effect of neurokinin1 receptor blockade on territorial aggression and in a model of violent aggression. *Biological psychiatry*. 2008; 63:271–278. [PubMed: 17678879]
34. Halasz J, et al. Substance P neurotransmission and violent aggression: the role of tachykinin NK(1) receptors in the hypothalamic attack area. *European journal of pharmacology*. 2009; 611:35–43. [PubMed: 19344710]
35. Slimko EM, McKinney S, Anderson DJ, Davidson N, Lester HA. Selective electrical silencing of mammalian neurons in vitro by the use of invertebrate ligand-gated chloride channels. *J Neurosci*. 2002; 22:7373–7379. [PubMed: 12196558]
36. Li P, Slimko EM, Lester HA. Selective elimination of glutamate activation and introduction of fluorescent proteins into a *Caenorhabditis elegans* chloride channel. *FEBS Letters*. 2002; 528:77–82. [PubMed: 12297283]
37. van der Poel AM, et al. A locked, non-rotating, completely embedded, moveable electrode for chronic brain stimulation studies in freely moving, fighting rats. *Physiology & behavior*. 1983; 31:259–263. [PubMed: 6685324]
38. Blanchard RJ, Wall PM, Blanchard DC. Problems in the study of rodent aggression. *Hormones and behavior*. 2003; 44:161–170. [PubMed: 14609538]
39. Lonstein JS, Gammie SC. Sensory, hormonal, and neural control of maternal aggression in laboratory rodents. *Neurosci Biobehav Rev*. 2002; 26:869–888. doi:S0149763402000878 [pii]. [PubMed: 12667494]
40. Kruk MR, et al. Comparison of aggressive behaviour induced by electrical stimulation in the hypothalamus of male and female rats. *Progress in brain research*. 1984; 61:303–314. [PubMed: 6543251]
41. Pfaff DW, Sakuma Y. Facilitation of the lordosis reflex of female rats from the ventromedial nucleus of the hypothalamus. *The Journal of physiology*. 1979; 288:189–202. [PubMed: 469715]
42. Pfaff DW, Sakuma Y. Deficit in the lordosis reflex of female rats caused by lesions in the ventromedial nucleus of the hypothalamus. *The Journal of physiology*. 1979; 288:203–210. [PubMed: 469716]

43. Petrovich GD, Canteras NS, Swanson LW. Combinatorial amygdalar inputs to hippocampal domains and hypothalamic behavior systems. *Brain Res Brain Res Rev*. 2001; 38:247–289. doi:S0165017301000807 [pii]. [PubMed: 11750934]
44. Mongeau R, Miller GA, Chiang E, Anderson DJ. Neural correlates of competing fear behaviors evoked by an innately aversive stimulus. *J Neurosci*. 2003; 23:3855–3868. [PubMed: 12736356]
45. Bragin A, et al. Multiple site silicon-based probes for chronic recordings in freely moving rats: implantation, recording and histological verification. *J Neurosci Methods*. 2000; 98:77–82. doi:S0165-0270(00)00193-X [pii]. [PubMed: 10837874]
46. Gradinaru V, Mogri M, Thompson KR, Henderson JM, Deisseroth K. Optical deconstruction of parkinsonian neural circuitry. *Science*. 2009; 324:354–359. doi:1167093 [pii]10.1126/science.1167093. [PubMed: 19299587]
47. Southwell AL, Ko J, Patterson PH. Intrabody gene therapy ameliorates motor, cognitive, and neuropathological symptoms in multiple mouse models of Huntington's disease. *J Neurosci*. 2009; 29:13589–13602. [PubMed: 19864571]



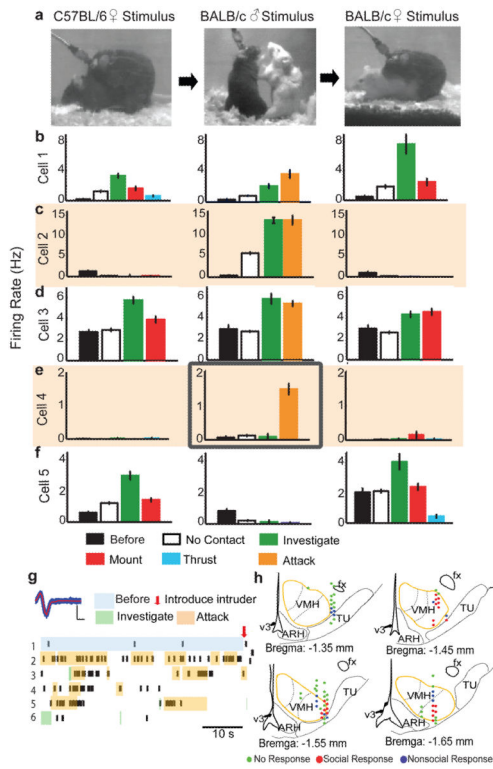


Figure 2. Response patterns of a VMHvl neuron during social encounters

a, Video frames taken from consecutive trials with intruder animals of the indicated sex and strain. **b-f**, Average firing rate during indicated behavioral episodes from 5 exemplar cells. “Before,” prior to introducing stimulus animal; “No contact,” periods during encounter without physical contact between intruder and resident . Error bars: \pm s.e.m. **g**, Recordings from the cell in (e) middle. Blue trace, superimposed individual spikes; red line, average spike shape. Scale bars: 200 μ V, 200 μ s. Raster plots illustrate 300 s of continuous recording. Colored shading and arrow mark manually annotated behavioral episodes. **h**, Schematics indicating cell response type at each recording site from Bregma level -1.35 mm to -1.65 mm. Anatomical structures based on Allen Brain Atlas (www.brain-map.org). fx: Fornix; ARH: Arcuate nucleus; v3: Third ventricle; TU: Tuberal nucleus.

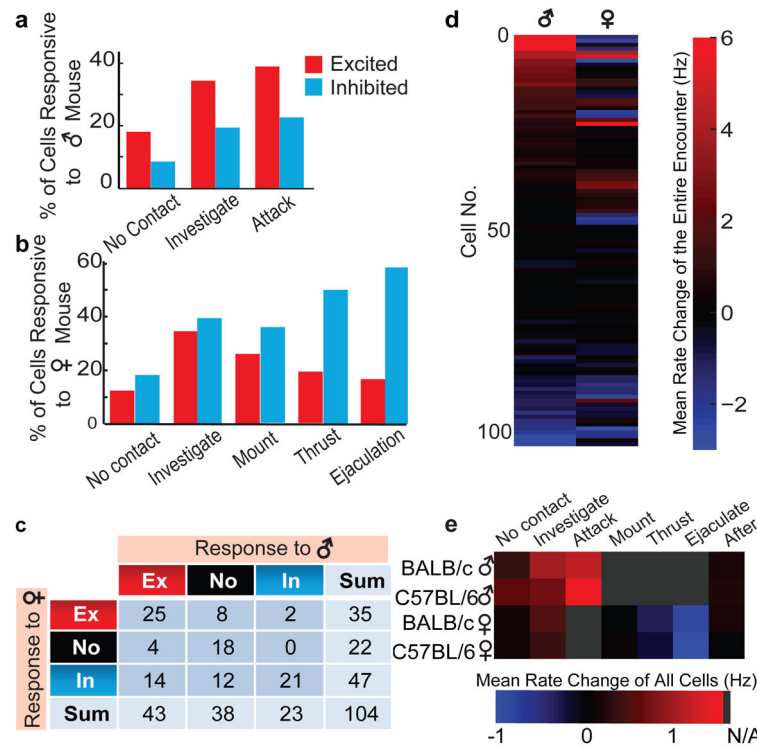


Figure 3. Summary of cell responses in VMHvl during mating and fighting

a, b, Percentage of cells excited (red) or inhibited (blue) during encounters with male (**a**) or female (**b**) mice. **c**, Numbers of cells exhibiting statistically significant changes in firing rate (see Methods online) towards males or females. **d**, Firing rate changes for all 104 recorded cells, averaged over entire encounter with males or females. **e**, Firing rate changes averaged over all 104 recorded cells, during various behavioral episodes. Gray, behavior not applicable (N/A) to the stimulus animal.

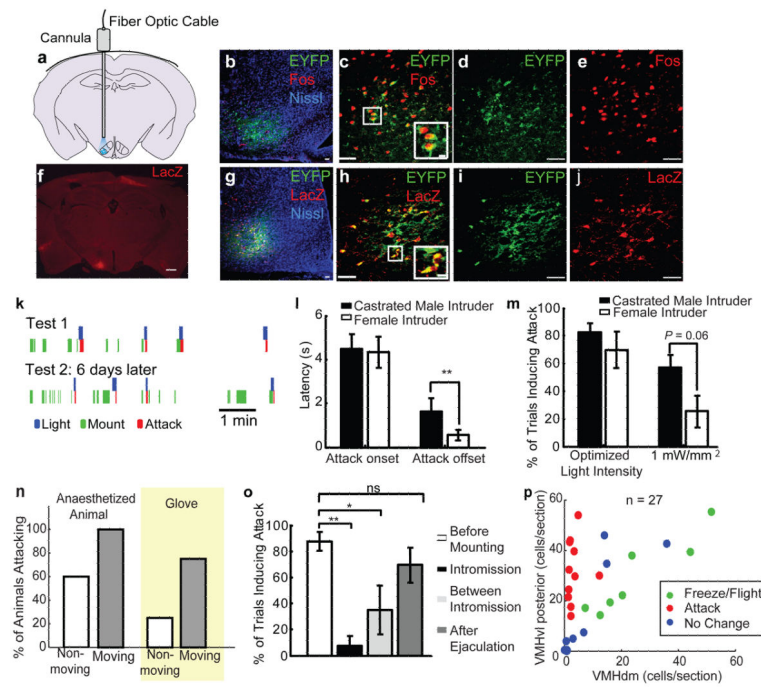


Figure 4. Optogenetic activation of VMHvl elicits attack in mice

a, Schematic illustrating optic fiber placement; VMHvl shaded in blue. **b-e**, Fos induction (red) in EF1α::ChR2-EYFP-expressing (green) cells at 1 hr post-illumination. Fos⁺ cells outside EYFP⁺ region may be synaptic targets of ChR2-activated cells. Blue: Fluorescent Nissl stain. **f**, LacZ expression identifies infected cell bodies (red). Scale bar: 500 μm. **g-j**, LacZ expression (red) and native ChR2-EYFP fluorescence (green) largely overlaps. Boxed areas in **c, h** enlarged at lower right. Scale bars in **(b-e, g-j)**: 50 μm or 10 μm (insets). **k**, Raster plots illustrating behavioral episodes (legend below) in a ChR2-expressing male paired with a female in 2 consecutive tests. **l**, Attack onset/offset latencies (relative to initiation vs. termination of illumination) towards indicated intruders **, $P < 0.01$. **m**, Efficacy of light-stimulated attack. “Optimized light intensity”: laser power yielding average maximal response in each animal (range: 1 - 3.3 mW/mm²). “1 mW/mm²”: average response obtained at this power. (t-test, $P = 0.06$). **n**, Percentage of animals attacking moving vs. non-moving anaesthetized animals or inflated glove (yellow shading). **o**, Percentage of trials inducing attacks towards female during successive stages of mating. * $P < 0.05$, ** $P < 0.01$ (One-way ANOVA with Bonferroni correction). **p**, Distribution of infected cells in each animal, plotted as cells per section in VMHvl posterior portion vs. that in (VMHdm + VMHc) region. Color code indicates whether illumination induced freeze/flight (green), attack (red) or no change in behavior (blue). See also Footnote S4 for further statistical analysis.

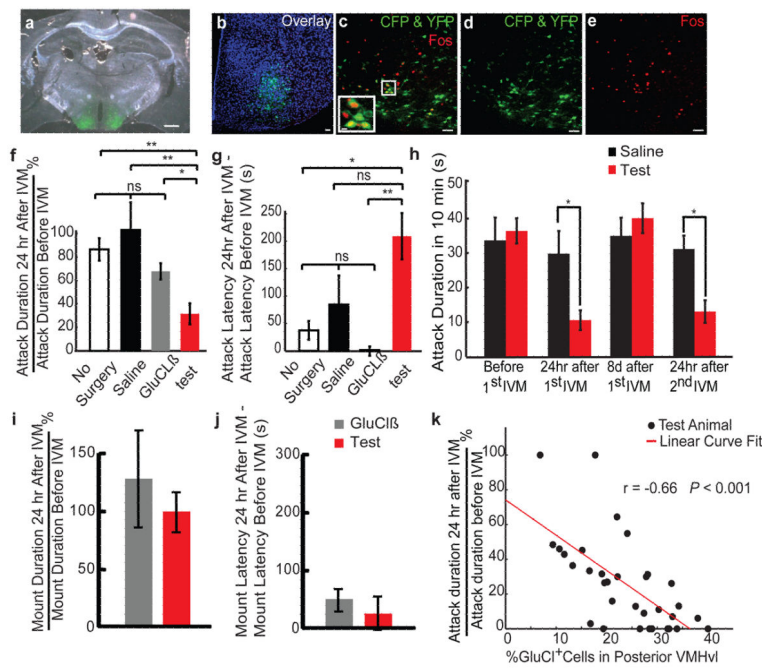


Figure 5. Reversible inhibition of natural aggression by genetic silencing of VMHvl

a, Anti-GFP antibody staining (green) in mice bilaterally infected with AAV2-GluCl α + AAV2-GluCl β . Scale bar: 500 μ m. **b-e**, Overlap between GluCl-expressing (green) and Fos-expressing (red) cells, 1hr after fighting. Blue: Topro-3 nuclear stain. Inset in (c) represents boxed area. Yellow cells are double-labeled. Scale bars: 50 μ m or 10 μ m (inset). **f, g**, Percent change in cumulative attack duration (**f**) and latency (**g**) during a 600 s resident-intruder trial before vs. 24 hr after IVM injection. Test: GluCl virus-injected animals (n = 33) (red bar). Control: no surgery (white bar, n = 12), saline (black bar, n = 6) or GluCl β virus-injected animals (n = 12, gray bar) (**, $P < 0.01$, *, $P < 0.05$, t-test). **h**, Cumulative attack duration during repeated cycles of IVM injection or washout (*, $P < 0.05$, Bonferroni posttests of two-way ANOVA with repeated measures). Test: GluCl virus-injected animals (n = 12); Control: Saline (n = 6). **i, j**, Percent change in mount duration (**i**) or latency (**j**) in test (n = 12) vs. control (GluCl β virus injected, n = 12) males paired with females. **k**, Percentage of infected cells in posterior portion of VMHvl (Bregma -1.4 mm — 1.8 mm) plotted against extent of aggression suppression after IVM injection. The Pearson correlation coefficient is significantly higher than 0 ($P < 0.001$). See Fig. S19 for further analysis.